Signal and Background Noise Photon Fluxes in a Coupling Electromagnetic Detecting System for High Frequency Gravitational Waves

(Response to Jason's Report)

Abstract

Unlike pure inverse Gertsenshtein effect (G-effect) caused by the high-frequency gravitational waves (HFGWs) in the GHz band, the electromagnetic (EM) detecting scheme (EDS) proposed by China and the US HFGW groups (2008) is based on the composite effect of the synchro-resonance effect and the inverse G-effect. The EDS is coupling system between a static magnetic field and a Gaussian beam (GB) and not the plane EM wave; key parameters in the EDS is first-order perturbative photon flux (PPF) and not second-order PPF; the distinguishable signal is the transverse first-order PPF and not the longitudinal PPF; the photon flux focused by the fractal membranes or other equivalent microwave lenses is total transverse flux and not only the transverse first-order PPF, but they have different signal-to-noise ratios at the different receiving surfaces. Theoretical analysis and numerical estimation show that the requisite minimal accumulation time of the signal at the special receiving surfaces and in the background noise fluctuation would be ~10^3-10^5 seconds and not huge cosmological time scale for the typical laboratory condition and parameters of $h_{rms} \sim 10^{-26} - 10^{-30} / \sqrt{\text{Hz}}$ and $\nu = 5\text{GHz}$.

1. The Gertsenshtein effect (G-effect) and its inverse effect.

It is well known that if an electromagnetic wave (EMW) propagates in a transverse homogeneous static magnetic field, it can generate the gravitational wave (GW). This is just the G-effect[1]. Then converting probability of the EMW (photons) into the GW (graviton) is given by [2,3] (in CGS units)

$$P \approx 4\pi G B^2 L^2 / c^4, \qquad (1.1)$$

where G is Newton's constant, B is the magnetic field. Contrarily, if a GW passes through a transverse homogeneous static magnetic field, then it can generate an EMW (photon flux), which propagates only in the same and in the opposite propagating directions of the GW. The latter is weaker than the former or is absent. This is just the pure inverse G-effect [3,4]. Whether the G-effect or its inverse effect, the conversion rate between the GWs (gravitons) and the EMWs (photons) is extremely low. For example, if B=10T=10^5Gauss, L=10m=1000cm, from Eq.(1), we have

$$P \approx 1.0 \times 10^{-32}. \qquad (1.2)$$

For the EM perturbative effect caused by the GWs in the EM fields, one's attention is often focused to the inverse G-effect. In order to consider the pure inverse G-effect in the laboratory size, the wavelength of GWs should be the comparable with the laboratory dimension. Thus the high-frequency GWs (HFGWs) in the microwave band (~10^8-10^{10}Hz) would be suitable researching object. In fact, physical foundation of the inverse G-effect is classical electrodynamics in curved spacetime. If a circular polarized HFGW passes through the transverse homogenous static magnetic field, according to the electrodynamical equations in curved spacetime, the EMW produced by the interaction of the HFGW with the static magnetic field can be given by [4,5] (in order to compare possible experimental effect, from now, we use MKS units.)

$$\vec{E}^{(1)} \approx A\hat{B}_y^{(0)} k_g cz \exp[i(k_g z - \omega_g t)], \quad (1.3)$$

$$\vec{B}^{(1)} \approx A\hat{B}_y^{(0)} k_g z \exp[i(k_g z - \omega_g t)], \quad (1.4)$$

where $\vec{E}^{(1)}$ and $\vec{B}^{(1)}$ are parallel to the xy-plane and $\vec{E}^{(1)} \perp \vec{B}^{(1)}$. Besides we assume $A = A_\oplus = A_\otimes = |h_\oplus| = |h_\otimes|$, they are the amplitudes of the HFGW with two polarization states, and the superscript (0) denotes the background EM fields, the notation ^ stands for the static EM fields, respectively. Here we neglected the EMW propagating along the negative direction of the z-axis, because it is often much less than the EM propagating along the positive direction of the z-axis. Eqs.(1.3) and (1.4) show that such perturbative EM fields have a space accumulation effect ($\propto z$) in the interacting region: this is because the GWs (gravitons) and EMWs (Photons) have the same propagating velocity, so that the two waves can generate an optimum coherent effect in the propagating direction [2,4]. From Eqs. (1.3) and (1.4), the power flux density of the EMW in the terminal receiving surface (z=L) will have maximum (z=L, see Figure 1)

$$u_{em} = 1/\mu_0 \cdot |\vec{E}^{(1)} \times \vec{B}^{(1)}| \approx 1/\mu_0 \cdot (A\hat{B}_y^{(0)} k_g L)^2 c. \quad (1.5)$$

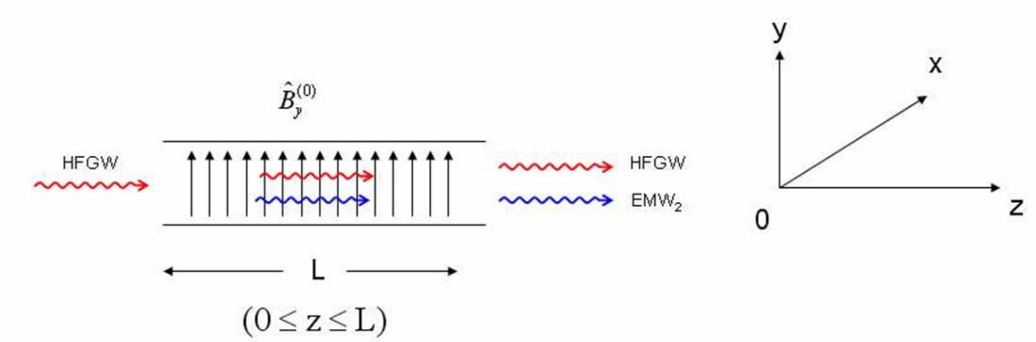

Figure1, If a HFGW passes through a static magnetic field $\vec{B}_y^{(0)}$, the interaction of the HFGW with the static magnetic field will produce an EMW, where L is the reacting region between the HFGW and the static magnetic field. The EMW_2 has maximum in the terminal position (Z=L) of the reacting region due to the space accumulation effect in the propagating direction the (z-direction).

In order to compare and analysis parameters introduced by Ref.[5,6], we choice following typical parameters in the references,

$$\hat{B}_y^{(0)} = 10\text{T}, \quad \text{L} = 10\text{m},$$

$$\nu_e = \nu_g = 5\text{GHz}\ (\lambda_g = 0.06m, k_e = k_g = \frac{2\pi}{\lambda} \approx 100),$$

$$h\nu = 3.3\times10^{-24} J\,(\text{energy of single photon}), \tag{1.6}$$

$$A \approx h_{rms} \approx \hat{h} = 10^{-26}/\sqrt{Hz} \text{ to } 10^{-30}/\sqrt{Hz},$$

$$\Delta s = 0.1\times0.1 = 0.01\text{m}^2 \text{ (typical receiving surface)},$$

where Δs is also the cross section of the interacting region. Then the total power flux passing through Δs in the terminal position (z=L) is

$$U_{em}^{(2)} = u_{em}\Delta s = \frac{1}{\mu_0}(A\hat{B}_y^{(0)} k_g L)^2 c\Delta s \approx 2.3\times10^{-40} W, \tag{1.7}$$

where the superscript (2) denotes the second-order perturbative EM power flux. Therefore, corresponding second-order perturbative photon flux (in quantum language) will be

$$N_\gamma^{(2)} = U_{em}^{(2)} / \hbar\omega_e \approx 2.3\times10^{-40} / 3.3\times10^{-24} \approx 7.0\times10^{-17} s^{-1}. \tag{1.8}$$

For the HFGW of $\nu_g = 5GHz$, $\hat{h} = 10^{-30}$, the total power flux passing through the Δs is given by [7]

$$U_{gw} = u_{gw}\Delta s = \frac{c^3}{8\pi G}\omega^2 A^2 \Delta s \approx 1.6\times 10^{-7} W, \qquad (1.9)$$

Thus corresponding graviton flux would be

$$N_g = U_{gw} / \hbar\omega \approx 4.8\times 10^{16} s^{-1}. \qquad (1.10)$$

Because the power fluxes, Eq.(1.7) (including the photon flux, Eq.(1.8)) is proportional to the amplitude squared of the HFGW, the second-order perturbative photon flux (PPF) exhibits a very small value.

From Eqs.(1.7)-(1.10), we obtain the conversion rate of the HFGW (gravitons) into the EMW (photons) as follows

$$P \approx U_{em} / U_{gw} = N_\gamma / N_g = \frac{2.3\times 10^{-40}}{1.6\times 10^{-7}} = \frac{7\times 10^{-17}}{4.8\times 10^{16}} \approx 1.4\times 10^{-33}. \qquad (1.11)$$

Eqs.(1.2) and (1.11) show that the conversion rates of the EMW (photons) into the HFGW (gravitons) and the contrary process have the close orders of magnitude. Thus, in order to obtain a second-order perturbative photon, from Eq. (1.8), the signal accumulation time would be, at least

$$\Delta t \approx 1/ N_r^{(2)} \approx \frac{1}{7\times 10^{-17}} \approx 1.4\times 10^{16}\text{s}. \qquad (1.12)$$

This is a very huge time interval. Eqs.(1.11) and (1.12) also show that the conversion rate of the HFGW (gravitons) into the EMW (photons) is extremely low. Thus the PPF in the pure inverse G-effect cannot cause a detectable signal and observable effect in the laboratory condition. Nevertheless, for some astrophysical and cosmological situations, it might cause interesting effect because very strong EM fields and GWs often occur simultaneously, and they distribute in the very big regions[8].

From Eqs. (1.5) (1.7),(1.8) and (1.12), one finds,

$$\begin{aligned} \text{if} \quad \hat{h} = 10^{-26}, \quad \text{then} \quad N_{\gamma}^{(2)} \approx 7\times10^{-9}\text{s}^{-1} \quad \text{and} \ \Delta t \approx 1.4\times10^{8}\text{s}, \\ \hat{h} = 10^{-24}, \quad \text{then} \quad N_{\gamma}^{(2)} \approx 7\times10^{-5}\text{s}^{-1} \quad \text{and} \ \Delta t \approx 1.4\times10^{4}\text{s}. \end{aligned} \tag{1.13}$$

Such results show that even if $\hat{h} = 10^{-24}$, it is still difficult to detect the HFGWs by the inverse G-effect in the laboratory condition. In other words, in order to generate an observable effect in such EM system, the amplitude of the HFGW of $\nu_g = 5GHz$ must be larger than $\hat{h} = 10^{-24}$, at least. Unfortunately, so far, for anything we know, perhaps there are no those HFGWs as strong as $\hat{h} = 10^{-24}$ or larger, although the EM system of the pure inverse G-effect in the high-vacuum and ultra-low-temperature condition has a very good low noise environment. Therefore, it is not utilizes by us in the HFGW detection.

2. Coupling between the static magnetic field and the plane EMW.

If a plane EMW and the HFGW pass through simultaneously the transverse homogenous static magnetic field, and the EMW and the HFGW have the same frequency, then the interaction of the HFGW with the static magnetic field and the EMW will generates the second-order perturbative EMW and the first-order perturbative EMW (the "interference term") (see Fig.2). We still assume the power of the background EMW is 10W, and it is limited in the cross section of $\Delta s = 0.1\times 0.1 = 0.01\text{m}^2$. Because the power flux of the plane EMW is distributed homogeneously in the cross section Δs, then

$$\left\langle P_{em} \right\rangle = \mathrm{Re}\left(\frac{1}{2\mu_0} E_x^{*(0)} B_y^{(0)} \right) \Delta s = \frac{1}{2\mu_0} \frac{E_x^{(0)^2}}{c} \Delta s = 10\mathrm{w}, \tag{2.1}$$

and $\quad |\vec{E}_x^{(0)}| \approx 8.7 \times 10^2 Vm^{-1}.$

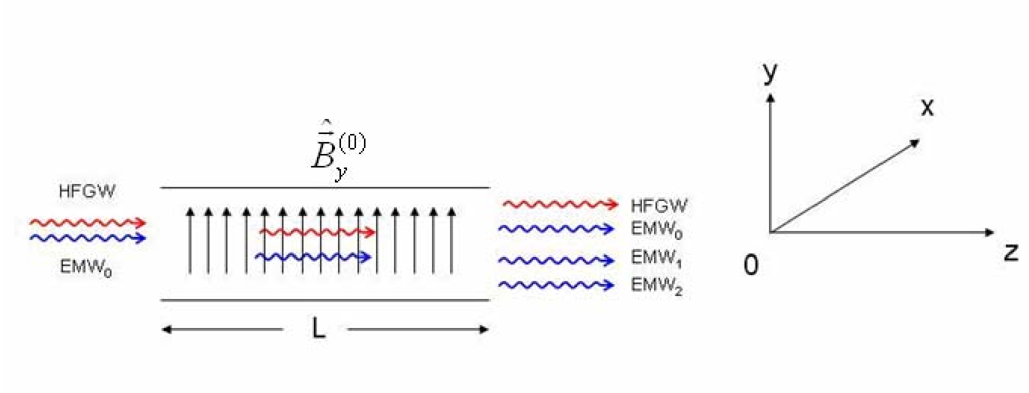

Figure 2. If the HFGW and the EMW_0 pass through simultaneously the transverse static magnetic field $\vec{B}_y^{(0)}$, under the resonant state ($\omega_g = \omega_e$), the first-order perturbative EMW (EMW_1, i.e., "the interference term") and the second-order perturbative EMW (the EMW_2) can be generated. However, because the EMW_1 and the EMW_0 have the same propagating direction and distribution, and EMW_1 is often much less than the EMW_0, the EMW_1 will be swamped by the EMW_0.

Total background photon flux passing through the cross section Δs will be

$$N_\gamma^{(0)} = 10 / \hbar\omega_e = \frac{10}{3.3 \times 10^{-24}} \approx 3.0 \times 10^{24} \mathrm{s}^{-1}. \tag{2.2}$$

Then corresponding first-order perturbative power flux in the z-direction

$$\begin{aligned} U_z^{(1)} &= \frac{1}{2\mu_0} [(\vec{E}^{(1)} \times \vec{B}_y^{(0)}) + (\vec{E}_x^{(0)} \times \vec{B}^{(1)})]_{\omega_e = \omega_g} \Delta s \\ &= \mathrm{Re}[\frac{1}{\mu_0} E^{(1)*} B_y^{(0)}] \cos\beta \cos\delta \cdot \Delta s \\ &= \mathrm{Re}[\frac{1}{\mu_0 c} E^{(1)*} E_x^{(0)}] \cos\beta \cos\delta \cdot \Delta s \\ &= \frac{1}{\mu_0 c} |\vec{E}^{(1)}| |\vec{E}_x^{(0)}| \cos\beta \cos\delta \cdot \Delta s \end{aligned}$$

where δ is the phase difference between the HFGW and the background EMW_0, β is the angle between $\vec{E}^{(1)}$ and $\vec{E}_x^{(0)}$ or $\vec{B}^{(1)}$ and $\vec{B}_y^{(0)}$, i.e. $\beta = \vec{E}_x^{(0)} \$ \vec{E}^{(1)} = \vec{B}_y^{(0)} \$ \vec{B}^{(1)}$, here $\delta = 0$ and $\beta = 0$ will always be possible by regulating the phase and the polarization directions of the background EMW_0. Then the HFGW and the EMW will have best matching state, i.e.,

$$U_z^{(1)}\Big|_{\substack{\delta=0\\ z=L}} = U_{z\,\max}^{(1)} = \mathrm{Re}[\frac{1}{\mu_0 c} E^{(1)*} E_x^{(0)}] \approx 6.9\times 10^{-20}\,\mathrm{w}. \tag{2.3}$$

Then the corresponding first-order PPF will be

$$N_z^{(1)} = U_z^{(1)} / \mathrm{h}\omega_e \approx 6.9\times 10^{-20} / 3.3\times 10^{-24} \approx 2.1\times 10^4 \mathrm{s}^{-1}. \tag{2.4}$$

Thus the total photon flux passing through Δs is about

$$N_z = N_z^{(0)} + N_z^{(1)} + N_z^{(2)} \approx (3.0\times 10^{24} + 2.1\times 10^4 + 7.0\times 10^{-17})\mathrm{s}^{-1}. \tag{2.5}$$

In this case the ratio of $N_z^{(1)}$ and $N_z^{(0)}$ is roughly

$$\sigma_1 = N_z^{(1)} / N_z^{(0)} \approx \frac{2.1\times 10^4}{3.0\times 10^{24}} \approx 7.0\times 10^{-21}, \tag{2.6}$$

This is also very small value and at the same time,

$$\sigma_2 = N_z^{(2)} / N_z^{(1)} \approx \frac{7.0\times 10^{-17}}{2.1\times 10^4} \approx 3.3\times 10^{-21}, \tag{2.7}$$

i.e., the second-order PPF is much less than the first-order PPF, while the first-order PPF is much less than the background photon flux (BPF). This means that if an EM detecting system contains simultaneously the static magnetic field and the EMW, then the interaction cross section between the GW (gravitons) and the EMW (photons) will be much larger than that in the pure inverse G-effect. The classical description and liner quantum theory for such property have a good self-consistency [2,9].

However, because the first-order PPF (signal) and the BPF (noise) have the same propagating direction and distribution, and the BPF is much larger than the PPF, so that the PPF will be swamped by the BPF. In this case the PPF has no direct observable effect. According to Eqs. (2.3) and (2.4), one finds

$$\begin{aligned} &\text{if } \hat{h} = 10^{-26}, \quad \text{then} \quad N_z^{(1)} \approx 2.1\times 10^{8}\,\mathrm{s}^{-1}, \\ &\text{if } \hat{h} = 10^{-25}, \quad \text{then} \quad N_z^{(1)} \approx 2.1\times 10^{9}\,\mathrm{s}^{-1}. \end{aligned} \tag{2.8}$$

For example, if $\hat{h} = 10^{-26}$, in order to displaying first-order PPF, $N_z^{(1)}\Delta t$ must be effectively larger than the background noise fluctuation $\sqrt{N_z^{(0)}\Delta t}$, i.e.,

$$\begin{aligned} &N_z^{(1)}(\Delta t)^{\frac{1}{2}} > \sqrt{N_z^{(0)}}, \\ &\text{then} \quad \Delta t > 6.8\times 10^{7}\,\mathrm{s}. \end{aligned} \tag{2.9}$$

Thus, detecting the HFGW of $\hat{h} = 10^{-26}$ and $\nu = 5GHz$ by such coupling EM system will also be very difficult.

3. Coupling system of the static magnetic field and the Gaussian Beam

Before we discuss the resonance effect of the HFGWs in the proposal EM system, we give a general analysis of the photon flux. Here, $\vec{E}^{(0)}, \vec{B}^{(0)}$ denote the background EM fields, $\vec{E}^{(1)}, \vec{B}^{(1)}$ the perturbative EM fields produced by the interaction of the HFGW with the static magnetic field. Then total EM power flux density is

$$\begin{aligned}\vec{u}_{em} &= \frac{1}{\mu_0}\vec{E}\times\vec{B} = \frac{1}{\mu_0}(\vec{E}^{(0)}+\vec{E}^{(1)})\times(\vec{B}^{(0)}+\vec{B}^{(1)}) \\ &= \frac{1}{\mu_0}\vec{E}^{(0)}\times\vec{B}^{(0)} + \frac{1}{\mu_0}(\vec{E}^{(0)}\times\vec{B}^{(1)}+\vec{E}^{(1)}\times\vec{B}^{(0)}) + \frac{1}{\mu_0}\vec{E}^{(1)}\times\vec{B}^{(1)}.\end{aligned} \tag{3.1}$$

Thus, the corresponding total photon flux density will be

$$\begin{aligned}\vec{n}_\gamma &= \frac{1}{\hbar\omega_e}\vec{u}_{em} \\ &= \frac{1}{\mu_0\hbar\omega_e}(\vec{E}^{(0)}\times\vec{B}^{(0)}) + \frac{1}{\mu_0\hbar\omega_e}(\vec{E}^{(0)}\times\vec{B}^{(1)}+\vec{E}^{(1)}\times\vec{B}^{(0)}) \\ &\quad + \frac{1}{\mu_0\hbar\omega_e}(\vec{E}^{(1)}\times\vec{B}^{(1)}) \\ &= \vec{n}^{(0)} + \vec{n}^{(1)} + \vec{n}^{(2)}\end{aligned} \tag{3.2}$$

where

$$\begin{aligned}\vec{n}^{(0)} &= \frac{1}{\mu_0\hbar\omega_e}(\vec{E}^{(0)}\times\vec{B}^{(0)}), \\ \vec{n}^{(1)} &= \frac{1}{\mu_0\hbar\omega_e}(\vec{E}^{(0)}\times\vec{B}^{(1)}+\vec{E}^{(1)}\times\vec{B}^{(0)}), \\ \vec{n}^{(2)} &= \frac{1}{\mu_0\hbar\omega_e}(\vec{E}^{(1)}\times\vec{B}^{(1)}).\end{aligned} \tag{3.3}$$

Eq.(3.2) and (3.3) would be most general form of the PPF and the BPF, where $\vec{n}^{(0)}$, $\vec{n}^{(1)}$ and $\vec{n}^{(2)}$ express the BPF, the first-order PPF and the second-order PPF densities, respectively. Since non-vanishing $|\vec{E}^{(0)}|, |\vec{B}^{(0)}|$ are often much larger than $|\vec{E}^{(1)}|, |\vec{B}^{(1)}|$, we have

$$|\vec{n}^{(0)}| ? \, |\vec{n}^{(1)}| ? \, |\vec{n}^{(2)}| . \qquad (3.4)$$

3-1.In the case of the plane EMW.

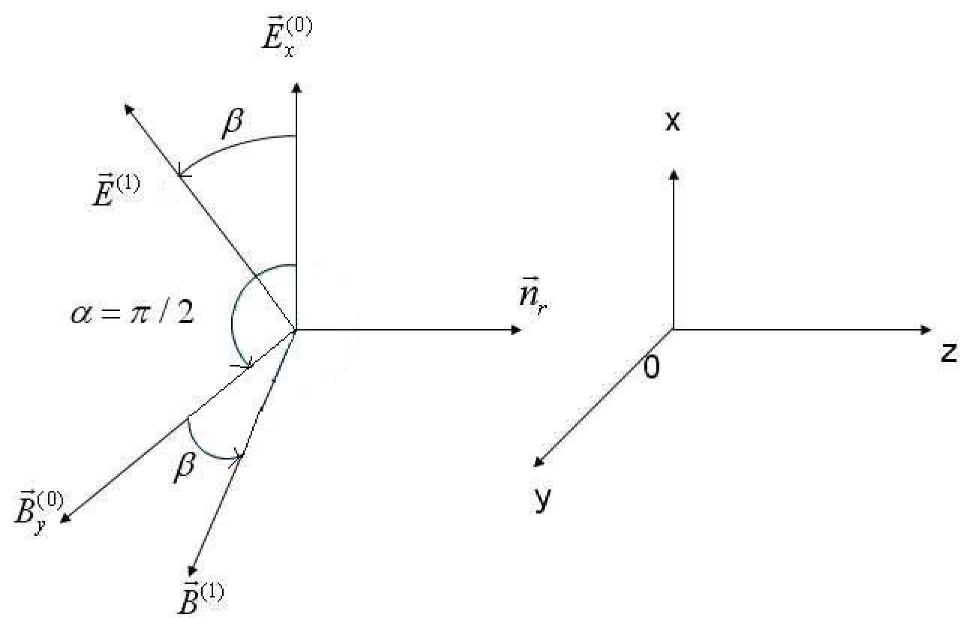

Figure 3. In the coupling system of the static magnetic field and the plane EMW, $|\vec{E}_x^{(0)}|$ and $|\vec{B}_y^{(0)}|$ denote the background EM field, $|\vec{E}^{(1)}|$ and $|\vec{B}^{(1)}|$ express the perturbative EM field generated by the direct interaction of the HFGW with the static magnetic field, $\vec{n}_\gamma$ is the total photon flux density.

If the HFGW and the plane EMW_0 all propagate along the z-direction, then Eq.(3-2) is deduced to (see Fig.3)

$$
\begin{aligned}
n_\gamma = \left\langle \vec{n}_\gamma \right\rangle_{\omega_e=\omega_g} &= \frac{1}{2\mu_0\hbar\omega_e}\left\langle (\vec{E}_x^{(0)} + \vec{E}^{(1)}) \times (\vec{B}_y^{(0)} + \vec{B}^{(1)}) \right\rangle_{\omega_e=\omega_g} \\
&= \frac{1}{2\mu_0\hbar\omega_e}\left\{ \left|\vec{E}_x^{(0)}\right|\left|\vec{B}_y^{(0)}\right| + \left[|\vec{E}_x^{(0)}||\vec{B}^{(1)}|\sin\left(\frac{\pi}{2}+\beta\right) \right.\right. \\
&\quad \left.\left. + |\vec{E}^{(1)}||\vec{B}_y^{(0)}|\sin\left(\frac{\pi}{2}-\beta\right) \right]\cos\delta + |\vec{E}^{(1)}||\vec{B}^{(1)}| \right\}
\end{aligned} \tag{3.5}
$$

where the angular bracket denotes the average over time. For the plane EMW in empty space, $B_y^{(0)} = E_x^{(0)}/c$, $B^{(1)} = E^{(1)}/c$ (in MKS units), then, Eq.(3-5) becomes

$$
\begin{aligned}
n_\gamma &= \frac{1}{2\mu_0 c\hbar\omega_e}\left\{ \left|\vec{E}_x^{(0)}\right|^2 + 2|\vec{E}_x^{(0)}||\vec{E}^{(1)}|\cos\beta\cos\delta + |\vec{E}^{(1)}|^2 \right\} \\
&= \frac{1}{2\mu_0 c\hbar\omega_e}\left\{ \left|\vec{E}_x^{(0)}\right|^2 + 2\vec{E}_x^{(0)}\cdot\vec{E}^{(1)}\cos\delta + |\vec{E}^{(1)}|^2 \right\} \\
&= n^{(0)} + n^{(1)} + n^{(2)},
\end{aligned} \tag{3.6}
$$

where

$$
\begin{aligned}
n^{(0)} &= \frac{1}{2\mu_0 c\hbar\omega_e}\left|\vec{E}_x^{(0)}\right|^2, \\
n^{(1)} &= \frac{1}{\mu_0 c\hbar\omega_e}\vec{E}_x^{(0)}\cdot\vec{E}^{(1)}\cos\delta, \\
n^{(2)} &= \frac{1}{2\mu_0 c\hbar\omega_e}|\vec{E}^{(1)}|^2 .
\end{aligned} \tag{3.7}
$$

In fact, Eq.(3.7) can also be expressed as

$$
\begin{aligned}
n^{(0)} &= \frac{1}{2\mu_0 c\hbar\omega_e}\left|\vec{E}_x^{(0)}\right|^2 = \dot{N}_0 \text{ (the background photon flux density)}, \\
n^{(2)} &= \frac{1}{2\mu_0 c\hbar\omega_e}|\vec{E}^{(1)}|^2 = \dot{N}_{GW} \text{ (the second-order PPF density)}.
\end{aligned} \tag{3.8}
$$

while

$$n^{(1)} = \frac{1}{\mu_0 c h \omega_e} \vec{E}_x^{(0)} \cdot \vec{E}^{(1)} \cos\delta = 2(\dot{N}_0 \dot{N}_{GW})^{\frac{1}{2}} \cos\delta = \dot{N}_1 \tag{3.9}$$

(the "interference term", i.e., the first-order PPF density).

Then, Eq.(3-6) can be re-written as

$$n_\gamma = \dot{N}_0 + 2(\dot{N}_0 \dot{N}_{GW})^{\frac{1}{2}} \cos\delta + \dot{N}_{GW}. \tag{3.10}$$

After a long time interval Δt the collected number of photons at the detector or at the receiving surface would be

$$N_d = n_\gamma \Delta t = \dot{N}_0 \Delta t + 2(\dot{N}_0 \dot{N}_{GW})^{\frac{1}{2}} \cos\delta \cdot \Delta t + \dot{N}_{GW} \Delta t. \tag{3.11}$$

This is just Eq.(3-32)in Ref.[6]. Clearly, in the plane EMW case, the BPF, the first-order PPF and the second-order PPF all propagate along the same direction, thus in any region and at any receiving surface

$$\dot{N}_0 \gg 2(\dot{N}_0 \dot{N}_{GW})^{\frac{1}{2}} \gg \dot{N}_{GW}, \tag{3.12}$$

is always valid. Thus, it is very difficult to display the first-order PPF effect ($n^{(1)} = 2(\dot{N}_0 \dot{N}_{GW})^{\frac{1}{2}} \cos\delta = \dot{N}_1$) in an accepted signal accumulation time interval and in the total photon flux.

Unlike the plane EM wave, however, the resonant response of the coupling system of the Gaussian beams (GB) and the static magnetic field to the HFGW will be much more complicated than that in the plane EM wave. In this case, the general expressions, Eqs.(3-2) and (3-3) are still valid. However, they will be expressed as the different concrete forms in the different directions and the receiving surfaces, and the relative relation between $n^{(0)}$ and $n^{(1)}$ would be different in the different receiving surfaces, even then they can reach up a comparable order of magnitude. This is worth consideration. The current coupling scheme [5] would be a useful candidate. Thus key parameters in the current scheme are the BPF and the first-order PPF in the special directions and not the photon number. The former are vectors and have high directivity. They decide the strength of the photon fluxes reaching the detector or the receiving surface, position and bearings of the detectors and the signal-to-noise ratio in the receiving surfaces.

3.2 Coupling system of the Gaussian Beam and the static magnetic field.

Unlike plane EMW, the GB has not only longitudinal BPF (the BPF in the z-direction) but also the transverse BPF, although the latter is often less than the former. Besides, the BPF in the transverse directions (e.g., the x- and y- direction) decays fast as the typical Gaussian decay rate. Thus in the some special regions and the directions, effect of both the PPF and the BPF would have a comparable order of magnitude.

For the GB with the double transverse polarized electric modes[5,10] it has

$$\begin{aligned} \vec{E}^{(0)} &= \vec{E}_x^{(0)} + \vec{E}_y^{(0)}, \\ \vec{B}^{(0)} &= \vec{B}_x^{(0)} + \vec{B}_y^{(0)} + \vec{B}_z^{(0)}. \end{aligned} \tag{3.13}$$

Such EM fields satisfy the Helmholtz equation. The non-vanishing perturbative EM fields are $\vec{E}_x^{(1)}, \vec{B}_y^{(1)}$ (the perturbative EM fields produced by the $\oplus$ polarization component of the HFGW) and $\vec{E}_y^{(1)}, \vec{B}_x^{(1)}$ (the perturbative EM fields generated by the $\otimes$ polarization component of the HFGW) in our scheme, respectively (see, Ref.[5]), i.e.,

$$\vec{E}^{(1)} = \vec{E}_x^{(1)} + \vec{E}_y^{(1)}, \qquad (3.14)$$
$$\vec{B}^{(1)} = \vec{B}_x^{(1)} + \vec{B}_y^{(1)}.$$

Then, Eq.(3-2) has following form

$$\begin{aligned}\vec{n}_\gamma &= \frac{1}{\mu_0 \hbar \omega_e} \vec{E} \times \vec{B} \\ &= \frac{1}{\mu_0 \hbar \omega_e} \left\{ \left(\vec{E}_x^{(0)} + \vec{E}_x^{(1)} + \vec{E}_y^{(0)} + \vec{E}_y^{(1)} \right) \times \left(\vec{B}_x^{(0)} + \vec{B}_x^{(1)} + \vec{B}_y^{(0)} + \vec{B}_y^{(1)} + \vec{B}_z^{(0)} \right) \right\}.\end{aligned} \qquad (3.15)$$

From Eq. (3-15), under the resonant state ($\omega_e = \omega_g$) the total photon flux densities in the z-direction (the longitudinal direction of the GB) and in the transverse direction (the x- and y- directions) can be given by

$$\begin{aligned}n_z = \frac{1}{2\mu_0 \hbar \omega_e} \mathrm{Re} \Big\{ &\left[E_x^{*(0)} B_y^{(0)} + E_y^{*(0)} B_x^{(0)} \right] \\ &+ \left[E_x^{*(0)} B_y^{(1)} + E_y^{*(0)} B_x^{(1)} + E_x^{*(1)} B_y^{(0)} + E_y^{*(1)} B_x^{(0)} \right] \\ &+ \left[E_x^{*(1)} B_y^{(1)} + E_y^{*(1)} B_x^{(1)} \right] \Big\} \\ = n_z^{(0)} + n_z^{(1)} + n_z^{(2)}& \\ = n_z^{(0)} + n_z^{(1)} + o(h^2),&\end{aligned} \qquad (3.16)$$

$$n_x = \frac{1}{2\mu_0 \hbar \omega_e} \mathrm{Re} \left[E_y^{*(0)} B_z^{(0)} + E_y^{*(1)} B_z^{(0)} \right] = n_x^{(0)} + n_x^{(1)}, \qquad (3.17)$$

$$n_y = \frac{1}{2\mu_0 \hbar \omega_e} \mathrm{Re} \left[E_x^{*(0)} B_z^{(0)} + E_x^{*(1)} B_z^{(0)} \right] = n_y^{(0)} + n_y^{(1)}. \qquad (3.18)$$

(1) The photon flux in the z-direction (the longitudinal direction of the GB)

From Eq. (3.16) and Refs.[5,10], we have

$$n_z^{(0)} = \left|n_z^{(0)}\right|_{\max} \exp(-\frac{2r^2}{w^2}), \quad n_z^{(1)} = \left|n_z^{(1)}\right|_{\max} \exp(-\frac{r^2}{w^2}), \qquad (3.19)$$

where r is the radial distance to the symmetrical axis (the z-axis) of the GB, w is the spot radius of the GB. Eq.(3-19) shows that $n_z^{(0)}$ decays by the typical Gaussian decay rate $\exp(-\frac{2r^2}{w^2})$, while $n_z^{(1)}$ decays by the factor $\exp(-\frac{r^2}{w^2})$, i.e., the decay rate of $n_z^{(1)}$ is slower than that of $n_z^{(0)}$. However, since $\left|n_z^{(0)}\right|_{\max}$? $\left|n_z^{(1)}\right|_{\max}$ in the almost of the regions, it is difficult to generate observable effect by $n_z^{(1)}$ in the regions. For the HFGW parameters of $\hat{h} = 10^{-30}$, $\nu = 5\text{GHz}$, only if $r \to 34\text{cm}$ (in the xy plane), $n_z^{(1)}$ has comparable order of magnitude with $n_z^{(0)}$. However, where $n_z^{(1)}$ and $n_z^{(0)}$ all are decayed to the very small undetectable value $n_z^{(1)} \sim n_z^{(0)} \sim 10^{-16}\text{s}^{-1}\text{m}^{-2}$.

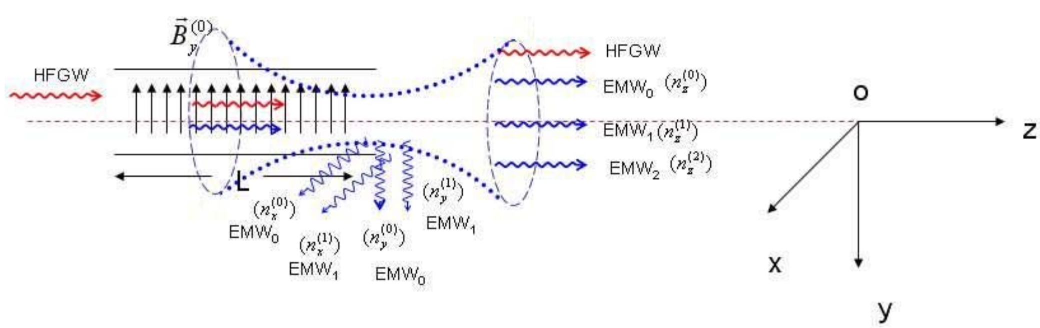

Figure 4. When the HFGW propagates along the z-direction in the coupling system of the GB and the transverse static magnetic field $\vec{B}_y^{(0)}$, the resonant interaction ($\omega_e = \omega_g$) of the HFGW with the EM fields will generate not only the longitudinal perturbative photon flux, but also the transverse perturbative photon fluxes ($n_x^{(1)}$ and $n_y^{(1)}$) in

the x- and y- directions due to the spread property of the GB itself. This is an important difference between Fig.2 and Fig.4. Moreover, unlike $n_z^{(1)}$ and $n_z^{(0)}$, $n_x^{(1)}$ and $n_x^{(0)}$ have very different distribution and the decay rate.

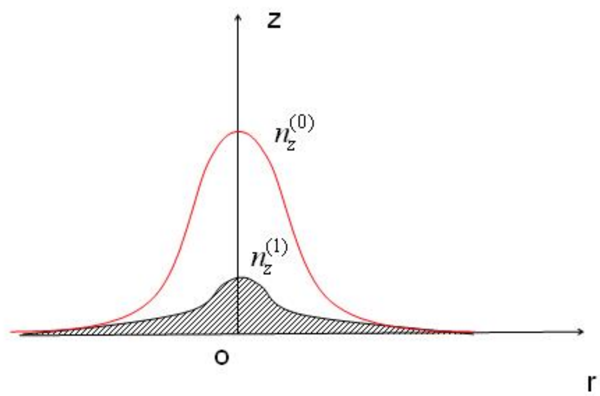

Figure 5, The first-order PPF density $n_z^{(1)}$ and the BPF density $n_z^{(0)}$ have the same propagating direction and the similar distribution. Thus $n_z^{(0)}$ is much larger than $n_z^{(1)}$ in most of the regions.

(2) The photon fluxes in the x-direction (the transverse direction of the GB).

According to Eq. (3.17), one finds

$$n_x = \frac{1}{2\mu_0 \hbar \omega_e} \left\langle |\vec{E}_y^{(0)}||\vec{B}_z^{(0)}| + |\vec{E}_y^{(1)}||\vec{B}_z^{(0)}| \cos\delta \right\rangle_{\omega_e=\omega_g}, \tag{3.20}$$

Setting $\delta = 0$ will always be possible by regulating the phase of the GB. Then (see Ref[5]).

$$\begin{aligned} n_x &= \frac{1}{2\mu_0 \hbar \omega_e} \left\{ \left\langle \vec{E}_y^{(0)} \vec{B}_z^{(0)} \right\rangle + \left\langle \vec{E}_y^{(1)} \vec{B}_z^{(0)} \right\rangle \right\}_{\omega_e=\omega_g} \\ &= n_x^{(0)} + n_x^{(1)} = \dot{N}_{0x} + \dot{N}_{1x} \end{aligned} \tag{3.21}$$

where

$$n_x^{(0)} = \dot{N}_{0x} = \frac{1}{2\mu_0 \hbar \omega_e}\left\langle \vec{E}_y^{(0)} \vec{B}_z^{(0)} \right\rangle = | n_x^{(0)} |_{\max}\ x \exp(-\frac{2x^2}{w^2}), \qquad (3.22)$$

$$n_x^{(1)} = \dot{N}_{1x} = \frac{1}{2\mu_0 \hbar \omega_e}\left\langle \vec{E}_y^{(1)} \vec{B}_z^{(0)} \right\rangle_{\omega_e = \omega_g} = \left| n_x^{(1)} \right|_{\max} \exp(-\frac{x^2}{w^2}), \qquad (3.23)$$

Unlike the case of plane EMW, Eqs. (3.22) and (3.33) show that $\dot{N}_{0x}$ will be not always larger than $\dot{N}_{1x}$. In the case of GB, $B_z^{(0)}$ of the GB depends not only on $\vec{E}_y^{(0)}$, but also $\vec{E}_x^{(0)}$, i.e.,

$$B_z^{(0)} = \frac{i}{\omega_e}(\frac{\partial E_x^{(0)}}{\partial y} - \frac{\partial E_y^{(0)}}{\partial x}). \qquad (3.24)$$

Therefore, when $E_y^{(0)} = 0$, $n_x^{(0)}$ must be vanish, but $n_x^{(1)} = n_{x\max}^{(1)} \neq 0$

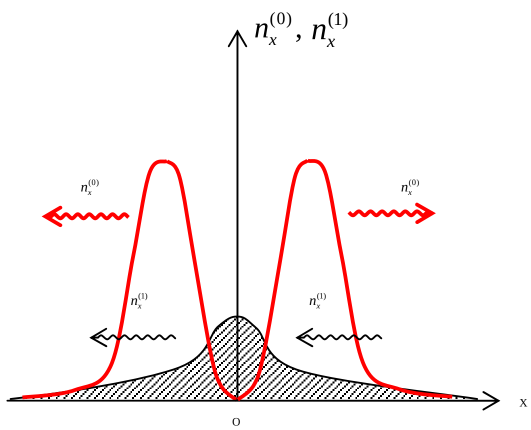

Figure 6. Schematic diagram of strength distribution of $n_x^{(0)}$ and $n_x^{(1)}$ in the "outgoing wave" region of the GB (another one is the "imploding wave" region. For an optimum GB, such properties of the transverse BPFs in such two regions would be anti-symmetric). Unlike Fig.5, here $n_x^{(0)}|_{x=0} = 0$ while $n_x^{(1)}|_{x=0} = n_x^{(1)}|_{\max}$. Therefore, $n_x^{(1)}\Delta t$ can be effectively larger than the background noise photon flux fluctuation $(n_x^{(0)}\Delta t)^{1/2}$, i.e., $n_x^{(1)}\Delta t > (n_x^{(0)}\Delta t)^{1/2}$ at the yz-plane and at the parallel surfaces near the yz-plane, and $n_x^{(1)}$ will be major fraction of the total transverse photon flux passing through the yz-plane, provided thermal photon flux and other noise photon fluxes passing through the surface can be effectively suppressed. Clearly, the EM response of the coupling system between the plane EMW and the static magnetic field has no such characteristic.

Although Eqs. (3.22) and (3.33) all represent the transverse photon fluxes in the x-direction, their physical behaviors are quite different:

(a) At the yz-plane $n_x^{(1)}|_{x=0} = n_x^{(1)}|_{\max}$ where $n_x^{(0)}|_{x=0} = 0$, i.e., the transverse PPF has a maximum at the longitudinal symmetrical surface of the GB where the transverse BPF vanishes. By the way, the transverse BPF at the longitudinal symmetrical surfaces being identically to zero is a fundamental characteristics of the GB's, whether the circular or elliptic GB's. Thus the transverse PPF would be major fraction of the total transverse photon fluxes flux passing through such surface provided the other noise photon flux passing through the surface can be effectively suppressed, although the PPF is much less than the BPF in other regions, and the PPF is always accompanied simultaneously by the BPF.

(b) The $n_x^{(1)}$ and $n_x^{(0)}$ have different decay rates in the x-direction, i.e., $n_x^{(1)} \propto \exp(-\frac{x^2}{\mathrm{w}^2}),\ n_x^{(0)} \propto x\exp(-\frac{2x^2}{\mathrm{w}^2})$ .The position of maximum of $n_x^{(1)}$ is the yz plane (x=0), while the position of maximum of $n_x^{(0)}$ is about x=3.2cm in our case. Thus, the signal-to-noise-ratio (SNR) $n_x^{(1)}/n_x^{(0)}$ will be very different at the different receiving surfaces. This means that it is always possible to obtain a best SNR $n_x^{(1)}/n_x^{(0)}$ by choosing the suitable region and the receiving surface. Using Eqs.(3.22) and (3.33), the total transverse photon fluxes passing through the receiving surface Δs can be given by

$$N_x^{(1)} = \int_{\Delta s} n_x^{(1)} ds, \tag{3.25}$$

$$N_x^{(0)} = \int_{\Delta s} n_x^{(0)} ds, \tag{3.26}$$

In the current scheme, $\Delta s \approx 10^{-2}\,\mathrm{m}^2$.

3.3 Numerical estimation of the transverse photon fluxes.

In order to measure the $N_x^{(1)}$ at a suitable receiving surface, $N_x^{(1)}\Delta t$ (notice that here $N_x^{(1)}$ is equivalent to $2(\dot{N}_0\dot{N}_{GW})^{\frac{1}{2}}$ in the plane EMW case, but both $N_x^{(1)}$ and $2\left(\dot{N}_0\dot{N}_{gw}\right)^{1/2}$ have a very different physical behavior) must be effectively larger than the noise photon fluctuation $(N_x^{(0)}\Delta t)^{1/2}$, i.e.,

$$N_x^{(1)}\Delta t > (N_x^{(0)}\Delta t)^{1/2}, \tag{3.27}$$

then

$$\Delta t > N_x^{(0)} / (N_x^{(1)})^2 = \Delta t_{\min}, \tag{3.28}$$

where $\Delta t_{\min}$ is requisite minimal signal accumulation time at the noise background $N_x^{(0)}$. In fact, Eqs. (3.27) and (3.28) are the concrete forms from the general relation Eqs. (3.2), (3.3) in the current scheme, while Eq. (2.9) is the concrete form from the general relation Eqs. (3.2) (3.3) in the plane EMW case. In the following we list the $N_x^{(1)}$, $N_x^{(0)}$, $\Delta t_{\min}$ and measurable HFGW strength $\hat{h}$ at the different receiving surfaces. If x=0 (the yz-plane), then $N_x^{(0)}$=0, it would be best measuring region for $N_x^{(1)}$. Of course, this does not mean that there are no other noise photon fluxes passing through the receiving surface Δs. In fact, scattering, diffraction and drift of the BPF and the thermal noise caused by the BPF all can generate smaller the noise photon fluxes passing through the surface Δs. Since they all caused by the BPF, they should have the same decay factor $\exp(-\frac{2x^2}{w^2})$ with the BPF. Moreover, external EM noise and the thermal noise caused by the environment temperature are independent of the BPF, but they can be effectively suppressed by high-quality Faraday cage or shielding covers, the low-temperature (T~ 1K or less) and vacuum operation. In general, they are much less than the BPF. Thus, our attention will be focused only on the BPF itself and the other noise photon flux $N_{x(other)}^{(0)}$ caused by the BPF. In this case, if such noise photon fluxes passing through the receiving surface Δs at the yz-plane can be limited a realizable level, then we can estimate the minimal signal accumulation time $\Delta t_{\min}$ in the noise background.

From the above discussion Eqs.(3.25),(3.26) and Ref.[5], the signal photon flux $N_x^{(1)}$ and the background photon flux $N_x^{(0)}$ passing through Δs are

$$N_x^{(1)} = \left|N_x^{(1)}\right|_{\max} \exp(-\frac{x^2}{w^2}), \tag{3.29}$$

$$N_x^{(0)} = \left|N_x^{(0)}\right|_{\max} x \exp(-\frac{2x^2}{w^2}), \tag{3.30}$$

and

$$N_{x(other)}^{(0)} = \left|N_{x(other)}^{(0)}\right|_{\max} \exp(-\frac{2x^2}{w^2}), \tag{3.31}$$

Displaying condition in the receiving surfaces will be

$$N_x^{(1)} \left(\Delta t\right)^{\frac{1}{2}} \geq \left[N_x^{(0)} + N_{x(\text{other})}^{(0)}\right]^{\frac{1}{2}}, \tag{3.32}$$

so

$$\Delta t \geq \frac{x\left|N_x^{(0)}\right|_{\max} + |\,N_{x(\text{other})}^{(0)}\,|_{\max}}{|\,N_x^{(1)}\,|_{\max}^2} \quad \text{and} \quad \Delta t_{\min} = \frac{x\left|N_x^{(0)}\right|_{\max} + |\,N_{x(\text{other})}^{(0)}\,|_{\max}}{|\,N_x^{(1)}\,|_{\max}^2}, \tag{3.33}$$

where $\left|N_x^{(0)}\right|_{\max} \approx 1.2\times 10^{22} s^{-1}$ in the typical parameters condition of the scheme. Then we can estimate $\Delta t_{\min}$ in the different parameters conditions.

(1) x=0, then $N_x^{(0)} \equiv 0$, from Eq.(3.33)

$$\Delta t_{\min} = \frac{|\,N_{x(\text{other})}^{(0)}\,|_{\max}}{|\,N_x^{(1)}\,|_{\max}^2}. \tag{3.34}$$

$\hat{h} = 10^{-30}$, then $N_x^{(1)} = |\,N_x^{(1)}\,|_{\max} \approx 4.6\times 10^3 \text{s}^{-1}$ and

$$\Delta t_{\min} \approx 3.0\times10^{3} s \quad \text{provided} \quad N^{(0)}_{x(\text{other})} < 6.3\times10^{10}\,\text{s}^{-1},$$

$$\Delta t_{\min} \approx 3.0\times10^{5} s \sim 3.5\text{days} \quad \text{provided} \quad N^{(0)}_{x(\text{other})} < 6.3\times10^{12}\,\text{s}^{-1} (\sim 21\text{PW}).$$

(3.35)

$\hat{h} = 10^{-26}$, then $|N^{(1)}_{x}|_{\max} \approx 4.6\times10^{7}\,\text{s}^{-1}$ and

$$\Delta t_{\min} \approx 3.0\times10^{3} s \quad \text{provided} \quad N^{(0)}_{x(\text{other})} < 6.3\times10^{18}\,\text{s}^{-1},$$

$$\Delta t_{\min} \approx 3.0\times10^{5} s \sim 3.5\text{days} \quad \text{provided} \quad N^{(0)}_{x(\text{other})} < 6.3\times10^{20}\,\text{s}^{-1}.$$

(3.36)

$\hat{h} = 10^{-25}$, then $|N^{(1)}_{x}|_{\max} \approx 4.6\times10^{8}\,\text{s}^{-1}$ and

$$\Delta t_{\min} \approx 3.0\times10^{3} s \quad \text{provided} \quad N^{(0)}_{x(\text{other})} < 6.3\times10^{20}\,\text{s}^{-1},$$

$$\Delta t_{\min} \approx 3.0\times10^{5} s \sim 3.5\text{days} \quad \text{provided} \quad N^{(0)}_{x(\text{other})} < 6.3\times10^{22}\,\text{s}^{-1}.$$

(3.37)

$\hat{h} = 10^{-24}$, then $|N^{(1)}_{x}|_{\max} \approx 4.6\times10^{9}\,\text{s}^{-1}$ and

$$\Delta t_{\min} \approx 3.0\times10^{3} s \quad \text{provided} \quad N^{(0)}_{x(\text{other})} < 6.3\times10^{22}\,\text{s}^{-1},$$

$$\Delta t_{\min} \approx 3.0\times10^{5} s \sim 3.5\text{days} \quad \text{provided} \quad N^{(0)}_{x(\text{other})} < 6.3\times10^{24}\,\text{s}^{-1}.$$

(3.38)

The above results show that limitation to the other noise photon fluxes passing through Δs would be very relaxed. It is interesting to compare Eqs. (2.9) and (3.36) they show that for the same parameter condition ($\hat{h} = 10^{-26}$, $\nu = 5\text{GHz}$), the current scheme have obvious advantages and reality.

(2) x=1cm=10^{-2}m, from Eq.(3.30), then $N^{(0)}_{x} \approx 1.1\times10^{20}\,\text{s}^{-1}$, but where $|N^{(0)}_{x(\text{other})}|_{\max}$ is often much less than $N^{(0)}_{x}$ i.e., $N^{(0)}_{x(\text{other})}$ can be neglected in the all following discussions.

$$\begin{aligned} &\hat{h} = 10^{-26}, \quad N^{(1)}_{x} \approx 4.4\times10^{7} s^{-1}, \quad \Delta t_{\min} \approx 5.7\times10^{4} s. \\ &\hat{h} = 10^{-25}, \quad N^{(1)}_{x} \approx 4.4\times10^{8} s^{-1}, \quad \Delta t_{\min} \approx 5.7\times10^{2} s. \\ &\hat{h} = 10^{-24}, \quad N^{(1)}_{x} \approx 4.4\times10^{9} s^{-1}, \quad \Delta t_{\min} \approx 5.7 s. \end{aligned} \tag{3.39}$$

(3) $x = 2cm = 2\times10^{-2}\,m$, then $N_x^{(0)} \approx 1.7\times10^{20}\,\text{s}^{-1}$

$$\begin{aligned}
&\hat{h} = 10^{-26}, \quad N_x^{(1)} \approx 3.9\times10^{7}\,\text{s}^{-1}, \quad \Delta t_{\min} \approx 1.1\times10^{5}\,s.\\
&\hat{h} = 10^{-25}, \quad N_x^{(1)} \approx 3.9\times10^{8}\,\text{s}^{-1}, \quad \Delta t_{\min} \approx 1.1\times10^{3}\,s.\\
&\hat{h} = 10^{-24}, \quad N_x^{(1)} \approx 3.9\times10^{9}\,\text{s}^{-1}, \quad \Delta t_{\min} \approx 1.1\times10 s.
\end{aligned} \tag{3.40}$$

(4) $x = 3cm = 3\times10^{-2}\,m$, then $N_x^{(0)} \approx 1.8\times10^{20}\,\text{s}^{-1}$

$$\begin{aligned}
&\hat{h} = 10^{-26}, \quad N_x^{(1)} \approx 3.2\times10^{7}\,\text{s}^{-1}, \quad \Delta t_{\min} \approx 1.7\times10^{5}\,s.\\
&\hat{h} = 10^{-25}, \quad N_x^{(1)} \approx 3.2\times10^{8}\,\text{s}^{-1}, \quad \Delta t_{\min} \approx 1.7\times10^{3}\,s.\\
&\hat{h} = 10^{-24}, \quad N_x^{(1)} \approx 3.2\times10^{9}\,\text{s}^{-1}, \quad \Delta t_{\min} \approx 1.7\times10 s.
\end{aligned} \tag{3.41}$$

(5) $x = 5cm = 5\times10^{-2}\,m$, then $N_x^{(0)} \approx 8.1\times10^{19}\,\text{s}^{-1}$

$$\begin{aligned}
&\hat{h} = 10^{-26}, \quad N_x^{(1)} \approx 1.7\times10^{7}\,\text{s}^{-1}, \quad \Delta t_{\min} \approx 2.8\times10^{6}\,s.\\
&\hat{h} = 10^{-25}, \quad N_x^{(1)} \approx 1.7\times10^{8}\,\text{s}^{-1}, \quad \Delta t_{\min} \approx 2.8\times10^{4}\,s.\\
&\hat{h} = 10^{-24}, \quad N_x^{(1)} \approx 1.7\times10^{9}\,\text{s}^{-1}, \quad \Delta t_{\min} \approx 2.8\times10^{2}\,s.
\end{aligned} \tag{3.42}$$

(6) $x = 10cm = 0.1m$, $N_x^{(0)} \approx 4.0\times10^{17}\,\text{s}^{-1}$

$$\begin{aligned}
&\hat{h} = 10^{-26}, \quad N_x^{(1)} \approx 8.4\times10^{5}\,s^{-1}, \quad \Delta t_{\min} \approx 5.6\times10^{5}\,s.\\
&\hat{h} = 10^{-25}, \quad N_x^{(1)} \approx 8.4\times10^{6}\,s^{-1}, \quad \Delta t_{\min} \approx 5.6\times10^{3}\,s.\\
&\hat{h} = 10^{-24}, \quad N_x^{(1)} \approx 8.4\times10^{7}\,s^{-1}, \quad \Delta t_{\min} \approx 5.6\times10 s.
\end{aligned} \tag{3.43}$$

(7) $x = 15\text{cm}$, $N_x^{(0)} \approx 2.7\times10^{13}\,\text{s}^{-1}$

$$\begin{aligned}
&\hat{h} = 10^{-26}, \quad N_x^{(1)} \approx 5.7\times10^{3}\,\text{s}^{-1}, \quad \Delta t_{\min} \approx 8.3\times10^{5}\,s.\\
&\hat{h} = 10^{-25}, \quad N_x^{(1)} \approx 5.7\times10^{4}\,\text{s}^{-1}, \quad \Delta t_{\min} \approx 8.3\times10^{3}\,s.\\
&\hat{h} = 10^{-24}, \quad N_x^{(1)} \approx 5.7\times10^{5}\,\text{s}^{-1}, \quad \Delta t_{\min} \approx 8.3\times10 s.
\end{aligned} \tag{3.44}$$

(8) $x = 20\text{cm}$, $N_x^{(0)} \approx 3.0\times10^{7}\,\text{s}^{-1}$

$$\hat{h} = 10^{-26}, \quad N_x^{(1)} \approx 5.2\text{s}^{-1}, \qquad \Delta t_{\min} \approx 1.1\times 10^6 s.$$
$$\hat{h} = 10^{-25}, \quad N_x^{(1)} \approx 5.2\times 10\text{s}^{-1}, \quad \Delta t_{\min} \approx 1.1\times 10^4 s. \tag{3.45}$$
$$\hat{h} = 10^{-24}, \quad N_x^{(1)} \approx 5.2\times 10^2\text{s}^{-1}, \quad \Delta t_{\min} \approx 1.1\times 10^2 s.$$

(9) $x = 28.3\text{cm}$, (about distance of 6 spot radiuses of the GB), $\hat{h} = 10^{-26}$, then $N_x^{(0)} \approx N_x^{(1)} \approx 6.3\times 10^{-7}\text{s}^{-1}$. Time of receiving one transversal photon would be $\Delta t_{\min} \approx \frac{1}{N_x^{(0)}} \approx \frac{1}{N_x^{(1)}} \approx \frac{1}{6.3\times 10^{-7}\text{s}^{-1}} = 1.6\times 10^6\text{s}$.

The above numerical estimation shows that:

(1) Best position displaying $N_x^{(1)}$ would be the yz-plane and the other parallel receiving surfaces in the region of $-2cm < x < 2cm$. In such regions, the transverse PPF $N_x^{(1)}$ for the parameter condition $\hat{h} \sim 10^{-24} - 10^{-30}$ may reach up to $\sim 4.6\times 10^9 s^{-1}$ to $4.6\times 10^3 s^{-1}$. If other noise photon fluxes passing through the surfaces can be effectively suppressed into $\sim 6.3\times 10^{24} s^{-1}$ to $\sim 6.3\times 10^{10} s^{-1}$, then corresponding minimal signal accumulation time $\Delta t_{\min}$ in the noise photon flux background would be $\sim 3\times 10^3 s$ to $6\times 10^5 s$.

(2) Unlike $N_x^{(1)}$, $N_x^{(0)}$ has maximum at $x \sim 3.2cm$, where $N_x^{(0)}$? $N_x^{(1)}$, but $N_x^{(1)}|_{x=3.2cm}$ and $N_x^{(1)}|_{x=0} = N_x^{(1)}|_{\max}$ have the same order of magnitude (e.g., if $\hat{h} = 10^{-26}$, then $N_x^{(1)}|_{x=0} = N_x^{(1)}|_{\max} \approx 4.6\times 10^7 s^{-1}$, $N_x^{(1)}|_{x=3.2cm} = 3.8\times 10^7 s^{-1}$). In the region, the detecting sensitivity would be worse 3-4 orders of magnitude than that at the yz-plane.

(3) Since $N_x^{(1)} = |N_x^{(1)}|_{\max} \exp(-\frac{x^2}{w^2})$, $N_x^{(0)} = |N_x^{(0)}|_{\max}\, x \exp(-\frac{2x^2}{w^2})$, even if $\hat{h} = 10^{-26}$, they will have the same order of magnitude in $x \approx 28\text{cm}$. However,

where $N_x^{(0)}, N_x^{(1)}$ all decayed to $\sim 6.3\times10^{-7}$ s^{-1}.

4. Role of fractal membranes

1) In the total above discussion, the proposal scheme did not involve the fractal membranes (FMs). In order words, even if we do not use the FM, above-mentioned relation between the PPF and the BPF is still valid. The FM is merely one of many possible ways to improve detecting quality. The fractal membranes in the GHz band have successfully been developed by the Hong Kong University of Science and Technology [11-13] from 2002-2005. Firstly, the fractal membranes (FMs) have very good selection ability to the photon fluxes in the GHz band. If the FM is nearly totally reflecting for the photon fluxes with certain frequencies in the GHz band, then it will be nearly total transmitting for the photon fluxes with other frequencies in the GHz band. Secondly, the FMs have good focus function to the photon fluxes in the GHz band. For example, the photon fluxes reflected and transmitted by the FMs can keep their strength invariant within the distance of 1 meter from the FMs. Such function has been proven by experimental tests. The role of the FMs in the scheme is only the reflector or the transmitter for the photon flux in the GHz band. Because $N_z^{(0)}, N_y^{(0)}$ and $N_x^{(0)}, N_x^{(1)}$ are exactly orthogonal for each other, an FM (or an equivalent microwave lens) paralleling with the yz-plane would focuses only $N_x^{(0)}, N_x^{(1)}$ and not $N_z^{(0)}, N_y^{(0)}$. In fact, here requirement for the FMs is also more relaxed, i.e., it does not require focusing the photon flux onto a micron-sized detector even into a point. In the typical parameter condition of the scheme, if the cross section of the focusing photon flux and the image size has the same or close size in the detector (in distance of ~28cm,) then the SNR $N_x^{(1)}/N_x^{(0)}$ at the receiving surface Δs and at the image surface $\Delta s'$ would be the same or close. Moreover, because unfocused $N_z^{(0)}, N_y^{(0)}$ will be decayed to 10^{-7}s^{-1} at x=28cm, it is possible to obtain better the SNR.

2) If the FM is just laid at the symmetrical plane (the yz-plane) or at the parallel planes very near the yz-plane, then the wave-fronts of the photon fluxes passing through the receiving surfaces Δs at the planes would be the plane or the pseudo-plane. Thus where it is possible to obtain a better focusing effect. The requirement for the focus in the region would be more relaxed than other regions. This is because such focusing quality depends on the local interaction of the photon fluxes at the receiving surfaces in the region of $|x| \leq 2cm$. Besides, provided the photon fluxes focused by the FM can keep a plane or pseudo-plane wave-front, then $N_x^{(0)}, N_x^{(1)}$ focused simultaneously on another surface $\Delta s'$ would have the same or the close SNR with that at Δs. Unique requirement for $N_x^{(1)}$ and $N_x^{(0)}$ at $\Delta s'$ is that $N_x^{(1)}(\Delta t)^{\frac{1}{2}}$ should be larger than $\sqrt{N_x^{(0)}}$ in a typical experimental time interval Δt, and this process does not need an image of high-quality at $\Delta s'$.

3) The photon fluxes $N_z^{(0)}$ and $N_z^{(1)}$ in the z-direction have the similar property. However, unlike relation between $N_x^{(0)}$ and $N_x^{(1)}$, $N_z^{(0)}$ (noise) is much larger than $N_z^{(1)}$ (signal) in the almost of all regions. This is a very important difference between the photon fluxes in such two directions.

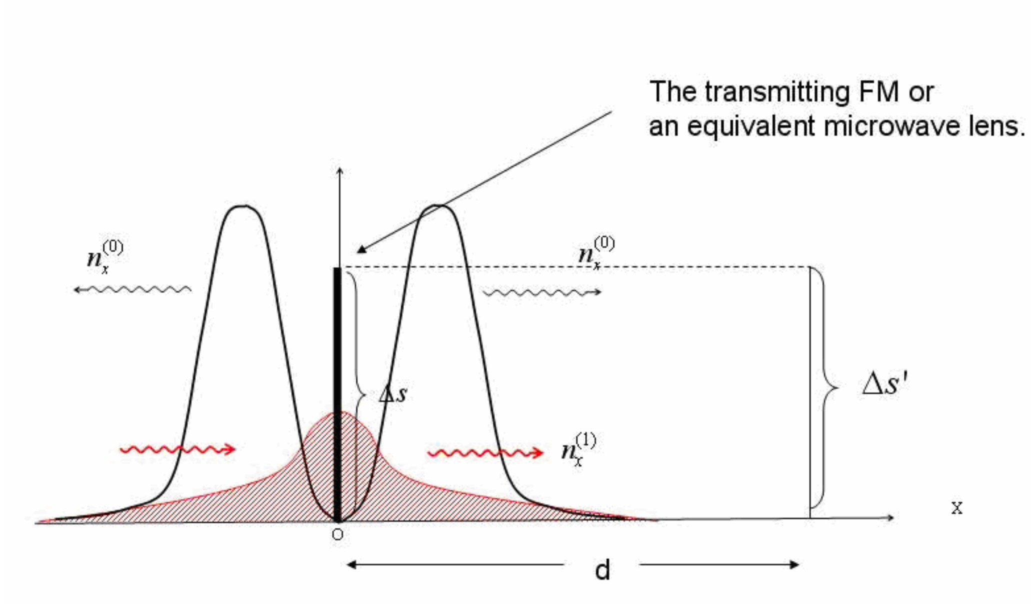

Figure7-(a)

Firgure7-(a): Unlike the photon fluxes $N_z^{(0)}, N_z^{(1)}$, $N_x^{(1)}|_{x=0} = N_x^{(1)}|_{\max}$ where $N_x^{(0)}|_{x=0} = 0$. This means that $N_x^{(0)}$ and $N_x^{(1)}$ focused by the FM at the yz-plane or at the parallel planes very near the yz-plane would have a good focusing effect and the SNR.

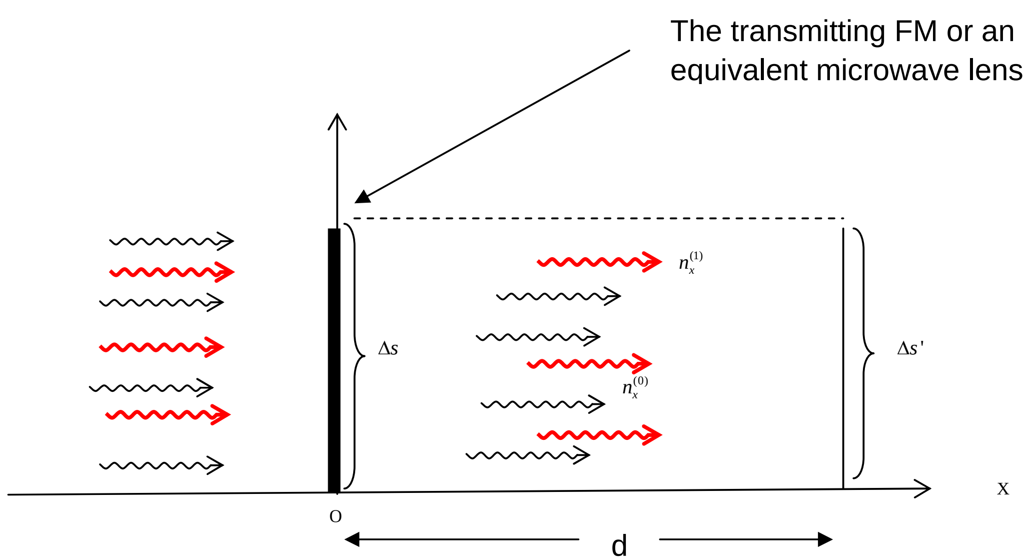

Figure7-(b),

Firgure7-(b): If the FM is just laid at the yz-plane or at the parallel planes very near the yz-plane, then the wave-fronts of the photon fluxes passing through the planes would be the plane or the pseudo-plane, and it is possible to obtain an effective focusing effect.

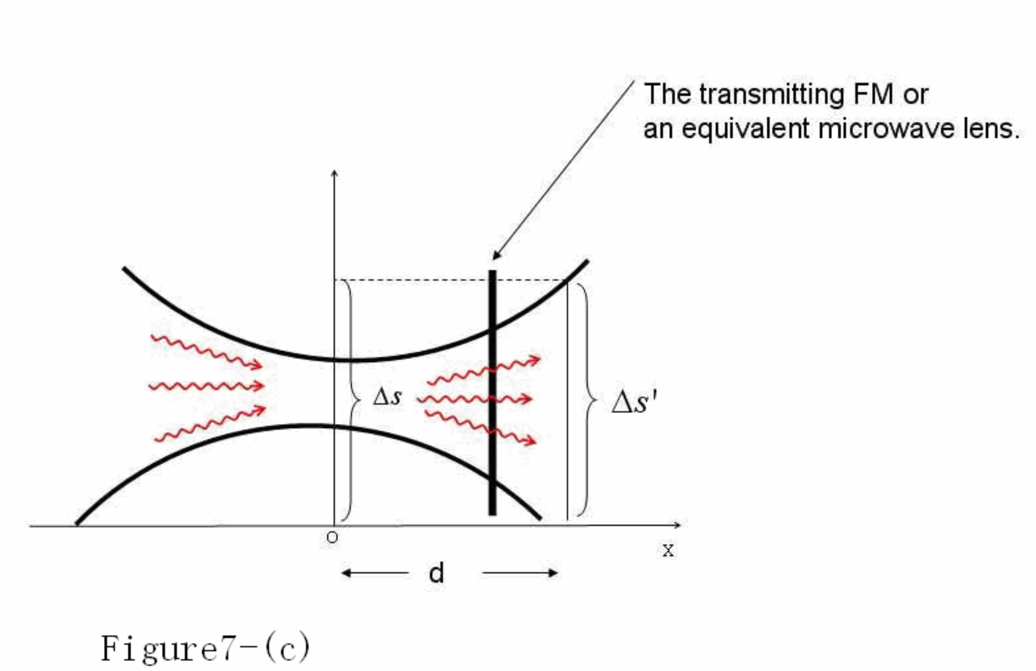

Firgure7-(c): If the FM is laid at an obvious non-symmetrical plane, then it is very difficult to focus the photon fluxes due to the spread property of the GB.

4) Such major role of the FM or other equivalent microwave lenses in the scheme is their focusing effect and not their superconductivity, and this does not mean that one can measure only $N_x^{(1)}$ ("interference term") and not $N^{(0)}$ (background). Also, it does not mean that $N^{(0)}$ is neglected and $N^{(0)}$ does not reach the photon flux detector. Actually, the FM is immersed in the BPF. Thus the BPF will generate the thermal noise in the FM. However, the BPF itself and the thermal noise photons caused by the BPF in the FM have essential difference. The former is vector and has high directivity; the latter are photons of random thermal motion. Under the low-temperature condition, the latter are much less than the former. Especially, $N_z^{(0)}, N_y^{(0)}$ of the BPF are exactly parallel to the yz-plane and exactly

perpendicular to $N_x^{(0)}$ and $N_x^{(1)}$. Thus $N_z^{(0)}$ and $N_y^{(0)}$ do not provide any direct contribution to the photon flux passing through the receiving surfaces paralleling to the yz plane, as well as they are not reflected, transmitted or focused by the FMs laying at the surface receiving surfaces. In other words, the photon flux focused by the FM will be $N_x^{(0)}, N_x^{(1)}$ and not $N_z^{(0)}, N_y^{(0)}$. In this case $N_x^{(1)}$ and $N_x^{(0)}$ would reach simultaneously the detector, but $N_x^{(1)}$ and $N_x^{(0)}$ in the different receiving surfaces have the different ratio $N_x^{(1)} / N_x^{(0)}$, this is an important difference to the plane EMW case. Therefore, it is always possible to choose a best region and the receiving surface to detect the total photon flux ($N_x^{(0)} + N_x^{(1)}$) which has a good signal-to-noise ratio.

5. Challenge and issues

Except for the above-principle analysis, of course, one must consider following challenge and issues. They would include the generation of high-quality GB, suppression of the thermal noise, the radiation press noise and noises caused by the scattering of photons and dielectric dissipation due to the dust and other particles, the thermal noise caused by the surface currents in the FM, etc.

The low-temperature (T~1K or less) and vacuum operation can effectively reduce the thermal noise and dielectric dissipation. Besides, there are large potential space and ways to improve the proposal scheme. They would include utilization of super-strong static magnetic field, matching of ultra-high sensitivity microwave photon detectors, construction of a good “microwave darkroom”, coupling between the open superconducting cavities and the current scheme (the open superconducting cavities have very large quantity factor Q~10^9-10^{11}, this coupling might greatly enhance the signal photon flux and not increase obviously the noise power), etc. All these issues need further theoretical study and careful experimental investigation, and they would provide new ways and possibility to further narrow the gap between the schemes and reality.

6. Brief summary

The proposal scheme (PS) is not based on the pure inverse Gertenshtein effect(G-effect) but the composite effect of the synchro-resonance effect and the inverse G-effect; PS is not coupling system between the plane EMW and the static magnetic field but the coupling between the Gaussian beam and the static magnetic field; key parameter in the PS is not the second-order PPF but the transverse first-order PPF; the measurable photon flux is not only the transverse first-order PPF but the total transverse photon flux, and they have different signal-to-noise ratios at the different receiving surfaces; the requisite minimal accumulation time Δt of the signal at the special receiving surface and in the background photon flux noise is not huge cosmological time scale but ~10^3-10^5 seconds for the parameter condition of $\hat{h} \sim 10^{-26} - 10^{-30}$ and $\nu = 5\text{GHz}$. This report does not involve the EM detection of the cavity to the HFGWs. We shall discuss and answer relative problems elsewhere.

References

[1] M.E.Gertsenshtein, Sov. Phys. JETP 14, 84 (1962)

[2] W.K.De Logi and A.R.Mickelson, Phys. Rev. D16, 2915(1977)

[3] A.N. Cillis and D.D. Harari, Phys. Rev. D54, 4757 (1996)

[4] D.Boccaletti et al., Nuovo CimB 70, 129(1970)

[5]F.Y.Li, R.M. L. Baker Jr., Z.Y. Fang, G.V. Stephenson and Z.Y. Chen, Http://arxiv.org/abs/0806,1989; The European Physical Journal c56, 407 (2008)

[6] JASON report, June 17 (2008),

[7] L.D. Landau and E.M. Lifshitz. The Classical Theory of Fields. (Nauka, Moscow) 1973, PP. 368-370

[8] P.Chen, Phys. Rev. Lett. 74, 634 (1995)

[9] V.De, Sabbata et al., Sov. J. Nucl. Phys. 8, 53-7 (1969)

[10] A. Yariv, Quantum Electronics 2nd ed, (Wiley, New York, 1975), P.110-129

[11] W.J.Wen et.al., Phys. Rev. Lett. 89, 223901 (2002)

[12] L.Zhou et al., Appt. Phys. Lett. 82, 1012 (2003)

[13] B. Hou et al., Opt. Express 13, 9149 (2005)